Quantum control of high harmonic generation in anharmonic potential

Muhamad Koyimatu[a,b], Kiyoshi Nishikawa[b]

[a]Faculty of Mathematics and Natural Sciences, Institut Teknologi Bandung, Jl. Ganesha 10, Bandung 40132 Indonesia, E-mail: s105koyimatu@mail.chem.itb.ac.id
[b]Institute of Science and Engineering, Kanazawa University, Kakuma, Kanazawa 920-1192 Japan, E-mail: kiyoshi@wriron1.s.kanazawa-u.ac.jp

Abstract.
In this work, we first aim to realize the high harmonic generation(HHG) spectrum in a classical and quantum treatment, and then to achieve the quantum control of the HHG spectrum. Here, we consider the HHG from the Duffing oscillator well-known as a typical anharmonic system. The HHG induced by the intense laser is a nonlinear optical process, where a molecular system absorbs n photons with energy $\hbar\omega$ and emits one high energy photon with energy $n\hbar\omega$. The light generated by HHG is a promising light source with an attosecond ultrashort pulse, which could be used to analyze the electronic structure and motion in molecule.
First, we perform a classical simulation to explain the structure of the HHG spectrum. Then, we investigate quantum-mechanically the mechanism of HHG, and compare the classical and quantum result. In quantum treatment, we apply the Fourier Grid Method (FGM) to obtain the eigenvalues and wavefuntion of the Duffing oscillator and use the Split Operator Method (SOM) to solve the time-dependent Schrödinger equation. Here we study the laser intensity dependence of the HHG with a single laser pulse, and then from the interference point of view, we focus on the role of the relative phase of two laser pulses and simulate to find out the phase dependence of the HHG. Finally we investigate the laser control of the HHG by changing the initial quantum state, which is a kind of a wave packet due to the superimposition of few eigenstates.

Keywords: HHG, SOM, anharmonic oscillator, quantum control

1 Introduction

Nonlinear optics process (NLOP) describes the response of the molecular system to the strong electromagnetic wave, and is usually induced only by a strong light such as a laser with high intensity. If the induced dipole moment of the material respond instantaneously to an applied electric field $E(t)$, the induced polarization $P(t)$ can be expressed in terms of the power of the electric field $E(t)$,

$$P(t) = \chi^{(1)}E(t) + \chi^{(2)}E^2(t) + \chi^{(3)}E^3(t) + \cdots . \tag{1}$$

Above perturbation treatment of the nonlinear optics could describe accurately the characteristics of the ordinary nonlinear optical phenomenon. With sufficiently intense laser field, the higher order terms play an very important role, and give rise to Fourier components of the polarization with high harmonics of the laser frequency, emitting the electromagnetic wave with the same frequency as the polarization. The harmonic generation is an interesting phenomenon, which describe a nonlinear process of light matter interaction, and a typical example of the process is a second-order harmonic generation.

Due to the great progress of the laser technique, an intense laser with the intensity $10^8 < I < 10^{12}$ W/cm^2 have become available, and we have discovered the noble interesting multi-photon processes in molecule [1], such as multi-photon absorption (MPA), multi-photon ionization (ATI), multi-photon dissociation (MPD), above threshold dissociation (ATD), the high harmonic generation (HHG), and so on, which are nonlinear optical processes arising from the higher-order effect of the external laser field.

Here we focus on the HHG, where a molecule absorbs n photons (with energy $\hbar\omega$) and emits one high photon with energy $n\hbar\omega$. HHG is experimentally observed by irradiating a noble gas with a near-IR laser pulse with a ultra high intensity 10^{14} W/cm^2, and the energy of the radiating electromagnetic wave is in the region of the extreme-ultraviolet (XUV) [2]. It have been known that the emitted photon energy is found to be the odd harmonics of the laser frequency $(2m+1)\hbar\omega$, and in some cases, the harmonic order $n = 2m + 1$ becomes larger than 100. The HHG spectrum has a characteristic structure, namely in a low energy region of HHG spectrum, the intensity of HHG rapidly decreases as the harmonic order increases, and then the typical harmonic shows a plateau, followed by a sharp cut-off. Thus the HHG provides an attractive light source of ultrashort coherent radiation in the XUV and soft-X-ray range, and it is expected that using the attosecond laser pulses by HHG, we could observe the electronic structure in molecule and control directly the motion of electron in molecule.

On the other hand, several theoretical methods have been developed to understand the basic mechanism of the HHG. Most familiar model is the sp-called three-step model by P.B.Corkum to explain semiclassically the basic generation mechanism of higher-order harmonics. Usually the potential induced by the ultrahigh intensity of the external oscillating field is comparable with the Coulomb potential due to the nucleus, so that electron moves in the deformed oscillating Coulomb potential, being a superposition of the Coloumb potential and the time dependent potential due to the laser field. When the intensity of the external field becomes close to the maximum, the electron go through the potential barrier by the tunneling ionization. Then the ionized electron is accelerated by the strong laser electric field, and acquire a lot of energy form the external field. Finally this accelerated ionized electron return back to the nucleus to recombine with it, emitting the high energy photon. Namely an electron emits the electromagnetic wave by three steps, i.e., (1) field induced tunnel ionization, (2) acceleration in the laser field, and (3) recombination and photoemission. Thus the energy of the emitted photon depends on the ionization potential of the atom and on the kinetic energy of the electron upon its return to its parent ion.

The paper is organized in the following way. In section 2,we develop the theoretical treatment, where we introduce the split operator method (SOM) to solve the time-dependent Scrödinger equation, and the Fourier grid Hamiltonian (FGH) method to solve the time-independent Scrödinger equation. In SOM, the time development operator $U(t)$ to generate the wavefunction $|\Psi(t)\rangle$ from the initial state $|\Psi(0\rangle)$ is an unitary transformation so that the norm of the wavefunction is always kept constant. Furthermore it uses the fast Fourier transformation (FFT), so that it solves the dynamics of the system in a very efficient way. On the other hand, FGH method is a effective way to solve the eigenvalue problem of the Hamiltonian matrix, and yields the eigenvalues and eigenvectors, which is required to construct the initial wavepacket for the quantum control of HHG. In section 3, we describe the details of the target Duffing oscillator, which is a typical anharmonic oscillator. The anharmonic term plays an fundamental role to generate the HHG. In section 4, we perform the classical simulation of the HHG, From the numerical solution of the Newton's equation, we estimate the dependence of the HHG spectra on the field intensity. In section 5, we develop the quantum mechanical treatment of the HHG, and calculate the HHG spectrum by changing the field intensity, and moreover investigate the relative phase dependence in the case of

the two color lase pulse. Finally we study the initial state dependence on HHG spectrum, where we adopt some initial wavepackets as a initial state. Last section treat the summary of this work.

2 Theoretical Treatments and Numerical Methods

2.1 Time-dependent Schrödinger Equation and Split Operator Method

Now we develop the semiclassical theory of the light-molecule interaction, where the molecular system is treated quantum-mechanically, but the electromagnetic filed is described by the time-dependent external field. Then the time-dependent Schrödinger equation is given by

$$i\hbar\frac{d}{dt}|\Psi(t)\rangle = [H_0 + V(t)]|\Psi(t)\rangle, \tag{2}$$

where H_0 and $V(t)$is the unperturbed molecular Hamiltonian and the perturbation Hamiltonian, respectively. In our simulation of the light-molecule interaction, the interaction Hamiltonian between the classical electronic field $\mathbf{E}(t)$ and the dipole moment operator $\boldsymbol{\mu}(r)$ is given by

$$V(t) = -\boldsymbol{\mu}(r)\cdot\mathbf{E}(t) \tag{3}$$

where the applied electric field $\mathbf{E}(t)$ is assumed as $\mathbf{E}(t) = \mathbf{E}_0 g(t)\sin(\omega t)$, where $\mathbf{E}_0$ and ω mean the amplitude vector and the frequency of the external electric field, and the shape function $g(t)$ of the laser pulse is assumed to be Gaussian function $g(t) = \mathrm{e}^{-(t-T_0)^2/\sigma^2}$, where T_0 and σ are the temporal center and the pulse width of the Gaussian pulse, respectively.

The time-dependent Schrödinger equation is generally solved by expanding the state ket $|\Phi(t)\rangle$ in terms of the eigenstate $|n\rangle$ of the molecular Hamiltonian H_0 for the set $\{|n\rangle|n = 0, 1, 2, \cdots\}$ is a complete orthonormal set, namely $|\Phi(t)\rangle = \sum_n C_n(t)|n\rangle$.

However, we here introduce the time-development operator $U(\Delta t)$ for the infinitesimal time increment Δt in order to analyze the dynamics of the time-dependent system. Then the formal solution of time dependent Schrödinger equation is given by

$$|\Psi(\Delta t)\rangle = U(\Delta t)|\Psi(0)\rangle, \tag{4}$$

where the infinitesimal time-development operator is given in terms of the total Hamiltonian H by $U(\Delta t) = \mathrm{e}^{-iH\Delta t/\hbar}$.

Here we divide the Hamiltonian operator into two parts *i.e.*, $H \equiv H_0 + V(t) = T + W(t)$. Note that the kinetic operator $T = p^2/2m$ and the potential term $W(t) = V_0 + V(t)$ does not commute. Now we employ the split operator method [3, 4] to solve the TDSE of the system numerically. The infinitesimal time-development operator is approximated by

$$\begin{aligned} U(\Delta t) &\equiv e^{-i(T+W)\Delta t/\hbar} &(5)\\ &\approx e^{-iW\Delta t/2\hbar}e^{-iT\Delta t/\hbar}e^{-iW\Delta t/2\hbar} + O(\Delta t^3). &(6)\end{aligned}$$

This approximation is correct up to the order Δt^3. Moreover, this approximated operator is unitary, so that the norm of the wavefunction obtained by applying this operator is kept constant while the numerical simulation. In order to get a state vector $|\Psi(t)\rangle$ at finite time t, we just apply this infinitesimal time-development operator to the initial state n-times, namely $|\Psi(t)\rangle = U(\Delta t)^n|\Psi(0)\rangle$, where n is the number of the simulation step, so the arbitrary time is given by $t = n\Delta t$.

In general, the wavefunction and the potential terms are diagonal in the coordinate space, and the kinetic operator is diagonal in the momentum space, Therefore we adopt the fast Fourier

transformation(FFT) in our numerical simulation, then we could effectively calculate the time-dependent wavefunction as follows;

$$\Psi(r, t_0 + \Delta t) \equiv \langle r|e^{-iW\Delta t/2\hbar}e^{-iT\Delta t/\hbar}e^{-iW\Delta t/2\hbar}|\Psi(t_0)\rangle \tag{7}$$

$$= e^{-iW(r,t_0)\Delta t/2\hbar}\mathrm{FFT}^{-1}[e^{-i\frac{p^2}{2m}\Delta t/\hbar}\mathrm{FFT}[e^{-iW(r,t_0)\Delta t/2\hbar}\Psi(r, t_0)]], \tag{8}$$

where the last line shows schematically the procedure of the programing, and FFT stand for the fast Fourier transform from the coordinate space to the momentum space, while FFT^{-1} represents the inverse FFT from the momentum space to the coordinate space.

2.2 Time-independent Schrödinger Equation and Fourier Grid Hamiltonian Method

In quantum simulation of the HHG, we need the wavefunction and the corresponding energy of the molecular system. In order to calculate correctly the eigenfunction and its energy in one and two dimensional systems, we here develop the Fourier Grid Hamiltonian(FGH) Method.

Now let us consider the general Hamiltonian H with a kinetic energy T and a local potential V (x). In actual numerical simulation, we adopt the discrete variable representation, namely, we discretize the coordinate variable to construct the Hamiltonian matrix, where every spatial point is described by the set $\{x_i = x_0 + (i-1)\Delta x \,|\, i = 1, 2, 3, \cdots, n\}$ and Δx is an spatial increment. We apply the second order differencing(SOD) to the 2nd-order spatial differenciation, then the explicit form of the matrix element for the kinetic and potential operator is given by, in the discretized coordination representation $\langle\langle x\rangle\rangle$,

$$T_{i,j} \equiv \langle x_i|\frac{p^2}{2m}|x_j\rangle = \frac{\hbar^2}{2m\Delta x^2}\{2\delta_{i,j} - \delta_{i,j+1} - \delta_{i,j+1a}\}, \tag{9}$$

$$V_{i,j} \equiv \langle x_i|V|x_j\rangle = V(x_i)\delta_{i,j}. \tag{10}$$

By means of the diagonalization of the Hamiltonian matirix $H_{i,j}$, we could obtain the eigenfunctions and eigenvalues of the system described by the Hamiltonian operator H. However, the accuracy of this method is mainly due to the evaluation of the kinetic operator, so we need a larger basis set to get a accurate results.

Now we develop the more efficient and accurate method called the Fourier Grid Hamiltonian(FGH) method. First we note that the kinetic operator is diagonal in the $\langle\langle p\rangle\rangle$ representation. Using the wavefunction of the momentum eigenstate $\langle x|p\rangle = e^{ipx}/\sqrt{2\pi}$, then the matrix element of the kinetic operator T is given by, in $\langle\langle x\rangle\rangle$ representation,

$$\langle x|T|y\rangle = \int dp\, \langle x|T|p\rangle\langle p|y\rangle = \frac{1}{2\pi}\int dp\, e^{-ip(x-y)}\frac{\hbar^2 p^2}{2m}. \tag{11}$$

This final expression means that this matrix element is given in terms of the Fourier transformation of the kinetic energy $(\hbar p)^2/2m$. Speaking exactly, p and q in above equation mean the wave vector, and we use this notation in the following.

Next we turn to the discrete variable representation, namely we introduce the discretized momentum basis set $\{|p_i\rangle \,|\, i = 1, 2, 3, \cdots, N\}$ in addition to the discretize coordinate basis set $\{|x_i\rangle \,|\, i = 1, 2, 3, \cdots, N\}$, where N means the dimension of the basis set, and usually is taken to be odd integer $N = 2n + 1$. Let the interval L of the coordinate under consideration be

$x_{min} \leq x \leq x_{max}$, so that $x_1 = x_{min}$ and $x_N = x_{max}$. Now we set $L = x_{max} - x_{min}$, then the spatial increment is $\Delta x = L/(N-1)$.

On the other hand, in the discretized momentum space, we could take the domain of the momentum as $0 \leq p \leq p_{max}$, where $p_1 = 0$ and $p_N = p_{max}$. Taking into account the periodicity in both spaces *i.e.*, $x_1 = x_{N+1}$ and $p_1 = p_{N+1}$ in the discrete Fourier transformation, the momentum increment Δp and maximum momentum p_{max} are given by in terms of Δx and N as $\Delta p = 2\pi/(N\Delta x)$. Each basis point of two spaces is given by $p_i = (i-1)\Delta p$ and $x_i = x_0 + (i-1)\Delta x$, however we could shift the domain of the momentum space due to the periodicity, namely we change the domain of the momentum point such as $-p_{max}/2 \leq p_i \leq p_{max}/2$.

Now we calculate the matrix element of kinetic operator in the discretized basis set,

$$\langle x_i|T|y_j\rangle = \frac{1}{2\pi}\sum_{l=-n}^{n} \Delta p\, e^{-ip_l(x_i-x_j)}\, T_l, \tag{12}$$

$$= \frac{1}{\Delta x}\sum_{l=1}^{n} \frac{2\mathrm{Cos}(2\pi l(i-j)/N)}{N}\, T_l, \tag{13}$$

where, for integer l, we define $T_l = (\hbar\Delta p)^2/(2m) \times l^2$. Thus we obtain the explicit form of the Hamiltonian matrix as

$$H_{i,j} = \frac{1}{\Delta x}\{\frac{2}{N}\sum_{l=1}^{n} \mathrm{Cos}(2\pi l(i-j)/N)\, T_l + V(x_i)\delta_{i,j}\}. \tag{14}$$

In this case, the Hamiltonian matrix $H_{i,j}\Delta x$ include more element than in the second-order differencing method, but a diagonalization of this Hamiltonian yield numerically more accurate result of the eigenvalues and eigenvectors.

3 Duffing Oscillator

The purpose of the paper is to present a detailed analysis of HHG by an anharmonic oscillator. Since HHG by noble gas atoms irradiated with intense laser pulses has been observed, the theory of the highly nonlinear optical processes has been developed to investigate the characteristic features of HHG spectrum, which consists of a first decrease, a long plateau, and a sharp cutoff. Many model atoms are studied to explain the characteristic response. Here we adopt the typical anharmonic oscillator with a quartic anharmonicity, so-called Duffing oscillator. The anharmonic oscillator generally presents several appealing properties to investigate the nonlinear dynamics of one dimensional systems, especially this allow us to make a comparison between the classical and quantum-mechanical treatments [5]. Thus we will show that we can be able to understand the some important aspects of HHG just by this very simple model.

The Duffing potential is written as

$$V(x) = \frac{1}{2}\,\omega_0^2\, x^2 + \frac{1}{4}\, v\, x^4, \tag{15}$$

where the first term represents the ordinary harmonic oscillator with the fundamental frequency ω_0, and the second one corresponds to the quartic anharmonicity with the anharmonic coefficient v. In this work, we restrict the motion of the electron to the bound state, namely we consider only the confining case $v > 0$.

Next, we turn to the quantum mechanical treatment of the Duffing oscillator. We calculate the wavefunction and the corresponding energy of the Duffing oscillator using the FGH method mentioned in the previous section. Here we used the parameter set $\{\omega_0 = 1, v = 5\}$. The resultant wavefunctions are used to construct the initial wavepacket of the HHG simulation in order to study the initial state dependence on the HHG spectrum, namely to investigate the quantum control of the HHG. Figure 1 shows the Duffing potential and five lowest wavefunctions.

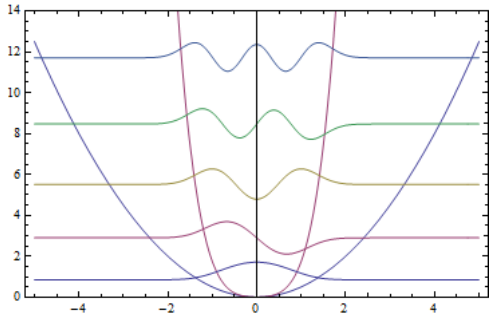

Figure 1: Plot of Duffing potential and wavefunction

In tis figure, the narrow quadratic curve means the Duffing potential, and the other one is the harmonic potential. The Duffing potential confines the electronic motion in the more narrow region. The behavior of the wavefunction of the Duffing oscillator is similar to the harmonic oscillator.

4 Classical Simulation

Here we develop the classical treatment of the HHG by the Duffing potential, so we investigate the classical motion of the electron in the quartic confining anharmonic oscillator under the intense electric field of the laser, $E(t) = E_0 \sin(\omega_1 t)$, where E_0 and ω_1 are the intensity and the frequency of the applied electric field, respectively. Then the total time-dependent potential of this system is given by

$$V(x,t) = \frac{1}{2}\,\omega_0^2\,x^2 + \frac{1}{4}\,v\,x^4 - ex\,E_0 \sin(\omega_1 t), \tag{16}$$

where the last term means the interaction of the electric field $E(t)$ and the electric dipole moment ex, and e is the charge of the electron. The harmonic frequency ω_0 is greater than the one of the external field ω_1, namely $\omega_0 > \omega_1$. This physically means that the electron doing fast motion due to the Duffing potential moves under the slowly oscillating potential.

In this model, we study not only the details of the HHG spectrum, but also the damping effect to the HHG spectrum. The quantum theory does not treat this damping effect, because there is no Hamiltonian to describe correctly the damping effect. Namely, the system with the damping term is dissipative and do not conserve the energy, but practically this effect is very important. Now consider the Newton's equation of motion with damping effect given by

$$\ddot{x} + \Gamma\,\dot{x} + \omega_0^2\,x + v\,x^3 = E_0 \sin(\omega_1 t), \tag{17}$$

where Γ is a damping coefficient. In order to analyze the oscillator dynamics given by the potential of Eq.16, we numerically integrate Eq.17. We assumed that the electron is rest at the origin at an initial time, namely we set the initial condition of the trajectory $x(t)$ as $\{x(0) = 0 \text{ and } \dot{x}(0) = 0\}$ to solve the second order differential equation.

As mentioned in the previous section, the power spectrum $I(\omega)$ is proportional to the absolute square of the Fourier transform of the acceleration $\alpha(t)$, i.e., $I(\omega) \propto |\alpha(\omega)|^2$. Thus in the following, we calculate $\alpha(\omega)$ to discuss the HHG spectrum. In the following, we will show the results of the HHG simulation in order to investigate the damping effect, the field intensity dependence, and the anharmonicity dependence to the HHG.

1. The damping effect on the HHG spectrum:

Here we show the typical example of the trajectory $x(t)$ and the related HHG spectrum, where the x-axis is the harmonic order $n = \omega/\omega_1$ In the following simulation we set the harmonic frequency $\omega_0 = 1$, namely we adopt this scaled unit. Here we used the parameters $\{v = 1, E_0 = 5, \text{and}\, \omega_1 = 0.1\}$. In figure 2, two trajctories $x(t)$ corresponding to the weak and strong damping cases and the harmonic oscillator without the damping ($v = 0 \,\text{and}\, \Gamma = 0$) are shown, and the corresponding HHG spectrum are shown in figure 3 The spectrum of the harmonic oscillator (without anharmonicity

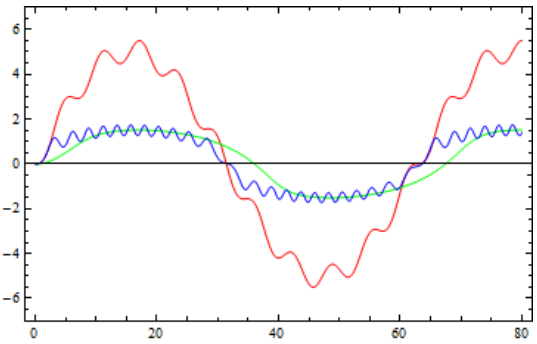

Figure 2: Time variation of trajectory $x(t)$ with respect to { Γ = 10(Green), 0.01(Blue), and harmonic oscillator (Red) }

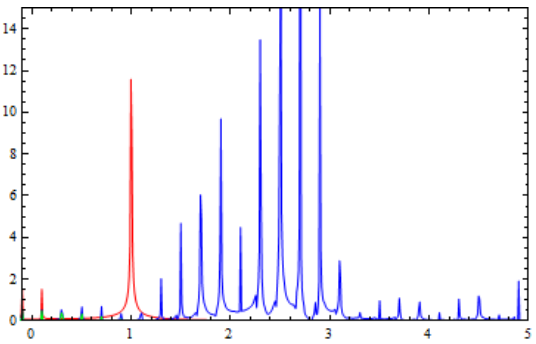

Figure 3: The corresponding HHG spectrum

and damping) shown by red peak in Fig.3 has only two peaks corresponding to the external frequency $\omega_1 = 0.1$ and the harmonic frequency $\omega_0 = 1$. The harmonic oscillator does not show any interesting optical response, while Duffing oscillator with the interaction of the electron and the field shows several peaks of the HHG, but for large damping suppress the HHG spectrum, i.e., there are small peaks (green) for $\Gamma = 10$. Therefore we are sure that the anharmonicity plays an very important role in the nonlinear optical response.

The amplitude of all trajectories if Fig.**??** have two frequency components of the periodic motion corresponding to ω_0 and ω_1. As the damping becomes large, the high frequency component of the $x(t)$ decrease, so that the largest damping $\Gamma = 10$ gives a smooth curve (green) and this behavior of the trajectory makes the HHG spectra disappear drastically. On the other hand,for small damping, several sharp spectrum peaks of the high harmonic order with $13 \leq n \leq 31$ appear.

2. Field intensity dependence:

In order study the intensity dependence, we set parameters $\{v = 5, \Gamma = 0.01, \text{and}\, \omega_1 = 0.1\}$, and we perform the simulation by changing the field intensity such as $E_0 = 1, 5, \text{and}\, 10$. As shown from Fig.4, as the field intensity increase, the amplitude of the trajectory also become large. For large field intensity, there appear the large ripple with the large amplitude corresponding to the high frequency component shown by blue curve in Fig.4. From the HHG spectrum shown in Fig.5,

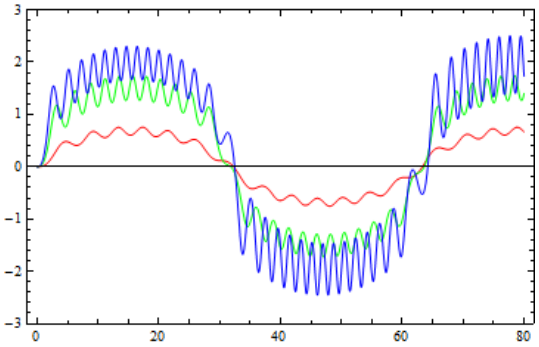

Figure 4: Time variation of trajectory $x(t)$ with respect to $\{E_0 = 1(\text{red}), 5(\text{green}), \text{and}\, 10(\text{Blue})\}$

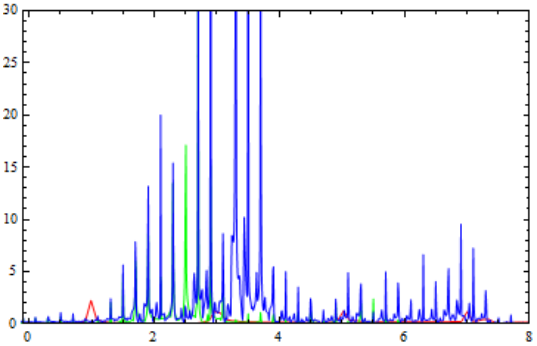

Figure 5: The corresponding HHG spectrum

we easily find out that as the intensity become large, both the intensity and the harmonic order of the HHG spectrum also become large. For strong field $E_0 = 10$ case, two peak groups appear around the harmonic order $15 < n < 40$ and $50 < n < 70$.

3. Anharmonicity dependence:

As we mentioned before, anharmonicity is very important to induce the HHG. In order to study the anharmonicity dependence, we set parameters $\{E_0 = 5, \Gamma = 0.01, \text{and}\, \omega_1 = 0.1\}$, and we perform the simulation by changing the anharmonicity coefficient such as $v = 0.1, 1, \text{and}\, 10$. Here we use the time variation of the acceleration $\alpha(t)$ instead of the trajectory $x(t)$. From the Fig.6, the behavior of the acceleration apparently looks like one of the trajectory, and as the anharmonicity becomes large, the high frequency component corresponding to the HHG shows the oscillation with more high frequency. While the low frequency component shows quite different behavior, namely the envelop of the large anharmonicity oscillate alternately with large and small amplitude. Fig.7 clearly shows that the global pattern of the HHG spectrum is similar for three cases, but its peaks shift to the high frequency (i.e., high harmonic order).

5 Quantum Simulation

Here, we develop the quantum mechanical treatment of the HHG. The time-dependent Schr—"odinger equation determines how a given initial wavefunction will change with time. It differs from Newton's law in two important ways: it involves a first time derivative instead of a second, and the square root of -1 appears explicitly in it. A wavefunction in an infinite square well is similar in some respects to a classical string clamped at both ends. In this section, we especially focus on the initial state dependence, the relative phase dependence in two color external field, and the interference effect on the HHG spectrum.

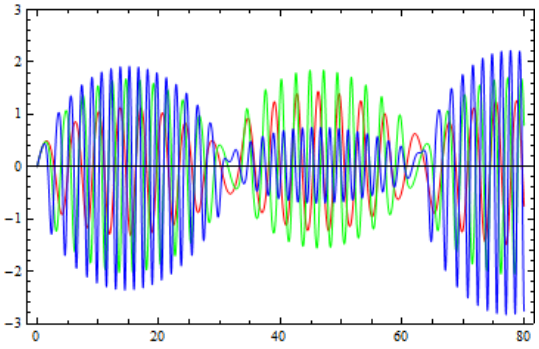

Figure 6: Time variation of acceleration $\alpha(t)$ with respect to $\{v = 0.1(\text{red}), 1(\text{green}), \text{and } 10(\text{Blue})\}$

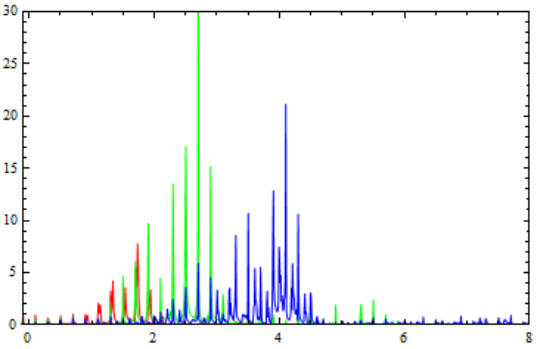

Figure 7: The corresponding HHG spectrum

1. Initial state dependence:

Initial wave function is calculated numerically by Fourier Grid Hamiltonian method, and we consider the lowest three states of the Duffing system, $\{\Psi_0, \Psi_1 \text{ and } \Psi_2\}$. By changing these initial wave functions, we make some quantum simulation and get the information about initial state dependence to HHG spectrum. Figure 8 show that we could see clearly some groups in the HHG

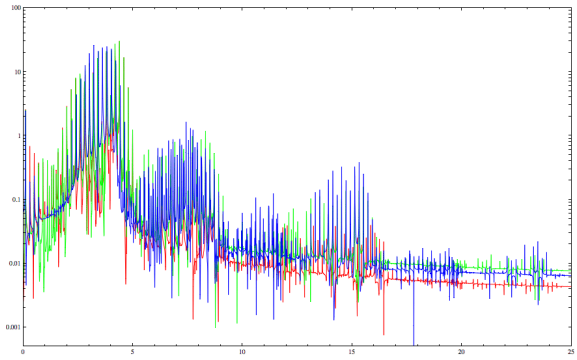

Figure 8: Initial state dependence on the HHG spectrum, where Ψ_0 (red), Ψ_1(green) and Ψ_2(blue)

spectrum peak, and in generally as the energy of the initial wave function becomes higher, the intensity of the give more intense HHG spectrum. But in the lowest region of the harmonic order, spectrum peaks from Ψ_0 and Ψ_1 is more intense, and the higher harmonic order region, the HHG pek groups from Ψ_2 look like more intense than Ψ_0 and Ψ_1.

2. Relative phase dependence of two-color laser pulses:

Next we performed the HHG simulation with a two-color laser, and examined the effect of the relative phase difference between two laser pulses. We here consider the following external field with two-color $\{\omega_1, 3\omega_1\}$,

$$\mathbf{E}(t) = \mathbf{E}_0 g(t) \left(\sin(\omega_1 t) + \sin(3\omega_1 t + \delta)\right), \tag{18}$$

where, δ is a relative phase of two laser pulses. The reason assuming the frequency of second pulse with three times the original pulse is that we expected the interference effect of two pathway by the two pulses in the HHG spectrum may occur. We observed the small difference in some peaks of the HHG spectrum, however we did not find out the drastic change of the some ports of the HHG spectrum due to the change of the relative phase of two pulses.

3. Analysis of interference effect:

Finally we have tried to control the HHG spectrum by using the wavepacket, which is a superposition of the three lowest states, $\{\Psi_0, \Psi_1 \text{ and } \Psi_2\}$. where we In this simulation we adopted the three states, $\{\psi_0, (\psi_0 + \psi_1)/\sqrt{2} \text{ and } (\psi_0 + \psi_1 + \psi_2)/\sqrt{3}\}$, as the initial state. If we consider the wavepacket made from three stationary states, then we could consider three pathway from three initial states to induce the HHG spectrum, and the HHG spectrum induced by three initial states could have a interference effect. Thus we have expected that the HHG spectrum from each component wavefunction constituting the wavepacket could make a interference, so that the HHG spectrum have a different structure from one of the each component wavefunction. The resultant HHG spectrum is shown Fig.9. The superposed initial state with higher energy gives stronger

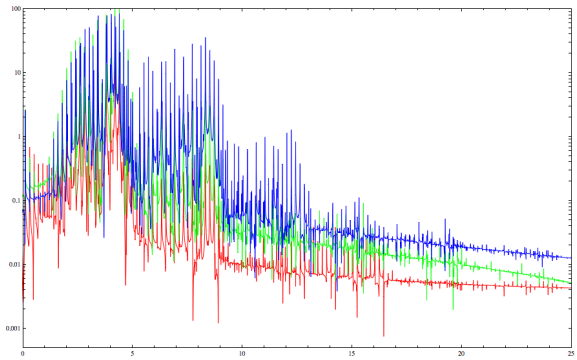

Figure 9: HHG spectrum from the superposed initial state, where Ψ_0(red),$(\Psi_0 + \Psi_1)/\sqrt{2}$(green) and $(\Psi_0 + \Psi_1 + \Psi_2)/\sqrt{3}$(blue)

HHG spectrum in almost all region except the lowest high harmonic order region.

Next we investigate the details of the difference due to the interference effect. In Figs.10 and 11, we show the averaged HHG spectrum (red curve) from two independent states and the HHG spectrum (blue curve) form the superposed state with interference effect. IN Fig.10, the red curve

show the averaged HHG spectrum with the initial state Ψ_0 and Ψ_1, and the blue curve is the spectrum of the superposed state $(\Psi_0 + \Psi_1)/\sqrt{2}$, while Fig.11 show the same spectrum related to the three initial states, Ψ_0, Ψ_1, and Ψ_2. We find clearly out that, in both cases, the intensity of the HHG spectrum from the wavepacket is larger than one of the averaged spectrum. However we could not realize the increase or decrease of spectrum peaks only with respect to the specified region. Namely it seems difficult to control only the specified peaks of the HHG spectrum.

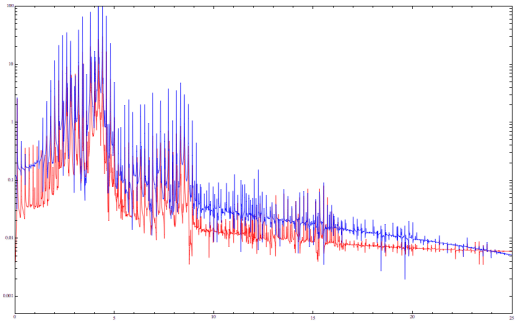

Figure 10: The averaged HHG spectrum from two states (res) and the HHG spectrum from the superposed state (blue)

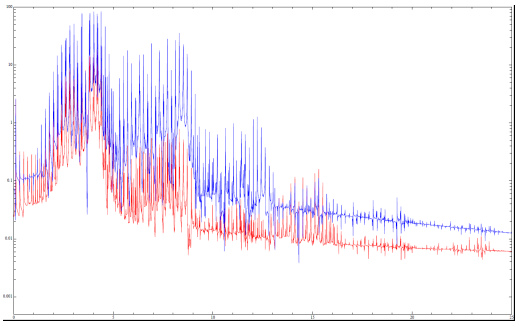

Figure 11: The interference effect for three-state case : the averaged HHG spectrum (red) and the HHG spectrum of the superposed state (blue)

6 Summary

The purpose of this work is to investigate the mechanism and spectrum of the high harmonic generation(HHG) in a classical and quantum-mechanical point of view, and finally we have made an simulation to achieve the quantum control of the HHG spectrum. Here, we considered the HHG from the Duffing oscillator well-known as a typical anharmonic system. HHG spectrum is calculated in terms of the Fourier transform of the acceleration $(\alpha(\omega))$.

In classical simulation, we have studied the damping effect, the intensity dependence, and the anharmonicity dependence on the HHG spectrum. In first simulation, we have found that the harmonic oscillator does not give rise to the nonlinear optical response, and then the large damping generates the weak HHG spectrum. Thus we understand that the anharmonicity is the fundamental quantity to induce the nonlinear optical response including HHG. Next by changing the field intensity and analyzing the time variation of the trajectory, we have clearly found that there are two oscillating components, corresponding to the harmonic (high) frequency ω_0 and the (low) frequency of external field ω_1. The HHG comes from the high frequency component, and the intense field yields the HHG with higher harmonic order. Then we have investigated the role of the anharmonicity. We have reconfirmed that as the anharmonic coefficient becomes large, the HHG spectrum with high harmonic order appears and the cut off energy increases.

In quantum simulation, we have studied the initial state dependence, the relative phase dependence in two color external field, and the interference effect on the HHG spectrum. First we have took the lowest three states of Duffing oscillator $\{|\Psi_0\rangle, |\Psi_1\rangle, \text{and}\, |\Psi_2\rangle\}$ as an initial state

$|\Psi(0)\rangle$, where we calculated the eigenfunctions and eigenvalues of Duffing oscillator by means of the FGH method. The initial state with more higher energy gives rise to the HHG spectrum with the more higher harmonic order. Next we performed the HHG simulation with a two-color laser, and examined the effect of the relative phase difference. However the change of the relative phase of two pulses does not show the clear difference on the HHG spectrum. Finally we have tried to control the HHG spectrum by using the wavepacket, where we adopted the three states $\{|\Psi_0\rangle, (|\Psi_0\rangle + |\Psi_1\rangle)/\sqrt{2}$, and $(|\Psi_0\rangle + |\Psi_1\rangle + |\Psi_2\rangle)/\sqrt{3}\}$ as the initial state $|\Psi(0)\rangle$. It is expected that the superposed state has many channel corresponding to each state to generate the HHG, and the HHG from some channel could give rise to the interference among some channels. From the resultant HHG spectrum, in almost all region, the superposed initial state with the higher energy state shows the stronger HHG spectrum, however, we could not find out clearly the interference effect. Namely three spectrum has almost the same shape, but we just found some peaks have a little difference in some region of the HHG spectrum.

Last I would like to comment on the mechanism of the HHG. In order to explain the HHG from the rare gas by the intense laser, P.B. Corkum proposed the three-step model, where the ionization and tunneling of the electron due to the deformation of the Coulomb attractive potential by the strong electric field of laser pulse plays an very fundamental role. However in the Duffing model only with the bound states, we could observe the HHG spectrum. From these simulation, it seems that the anharmonicity is the fundamental quantity to induce the nonlinear optical response.

References

[1] P. B. Corkum (1993). Plasma perpective on strong field multiphoton ionization. *J. Phys. Rev. A*, **71**, 1994 – 1997

[2] C. Winderfeld, Ch. Spielmann, and G. Gerber (2008). Optimal control of high-harmonic generation. *Rev. Mod. Phys.*, **80**, 117 – 140

[3] M.D. Feit, J.A. Fleck Jr. and A. Steiger (1982). Solution of the Schrödinger equation by a spectral method. *J. Comp. Phys.*, **47**, 412 – 433

[4] M. D. Feit and J. A. Fleck (1983). Solution of the Schrödinger equation by a spectral method II: Vibrational energy levels of triatomic molecules[a)]. *J. CHem. Phys.*, **78**, 301 – 308

[5] Ph. Balcou, Anne L'Huillier, and D. Escande (1996). High-order harmonic generation processes in classical and quantum anharmonic oscillators. *J. Phys. Rev. A* , **53**, 3456 – 3468